Amplified Luminescence in Organo-Curium Nanocrystal Hybrids

SCHOLARONE™
Manuscripts

COMMUNICATION

Amplified Luminescence in Organo-Curium Nanocrystal Hybrids

Peter Agbo,[a] Alexander Müller,[b] Leticia Arnedo-Sanchez,[a] Peter Ercius,[b] Andrew M. Minor,[b,c] and Rebecca J. Abergel*[,a,d]

We present the first report of ligand-sensitized actinide luminescence in a lanthanide nanoparticle host. Amplified luminescence of $^{248}Cm^{3+}$ doped in a $NaGdF_4$ lattice is achieved through optical pumping of a surface-localized metal chelator, 3,4,3-LI(1,2-HOPO), capable of sensitizing Cm^{3+} excited states. The data suggest the possibility of using such materials in theranostic applications, with a ligand-sensitized actinide or radio-lanthanide serving the dual roles of a nuclear decay source for radiotherapeutics, and as a luminescent center or energy transfer conduit to another emissive metal ion, for biological imaging.

The exploration of lanthanide luminescence in nanoparticle structures over the last decade has found much of its motivation behind their potential use in lasing, spectral conversion and biomedical imaging applications.[1-6] The result has been a broad body of literature produced in the areas of sensitized lanthanide luminescence, lanthanide spectral conversion, and actinide photospectroscopy in lanthanide host materials.[3, 6-13] Additionally, significant investigations have delved into creating *f*-element materials capable of serving the dual purpose of targeted radiotherapeutics and photoluminescent cell/tissue-imaging agents.[1, 14-17] Less work has considered the prospect of combining these research areas, through the synthesis of ligand-sensitized lanthanide nanoparticles with highly radioactive actinide co-dopants for radiotherapy applications. The dearth of research in this area motivated an investigation into the luminescent properties of curium-doped $NaGdF_4$ nanoparticles featuring a surface-bound chelator, 3,4,3-LI(1,2-HOPO),[18] hereafter 3,4,3 (Figure 1). This

study marks the first of its kind, with an actinide successfully doped into the hexagonal $NaGd(Y)F_4$-type lattices that have become common host crystals for solid-state lanthanide luminescence studies. Nanoparticles were synthesized from metal acetate precursors in a 1-oleic acid/1-octadecene mixture and were decorated with 3,4,3 by substitution of 1-oleate ligands, following methods adapted from the literature.[19] While we use a low-activity ^{248}Cm isotope for the sake of safety, these results should be applicable to the more radioactive ^{243}Cm and ^{244}Cm, if not other actinides and lanthanide isotopes as well.
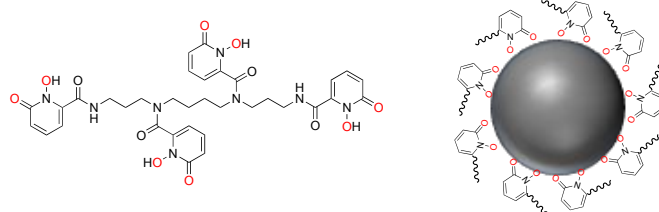
Figure 1. (left) Molecular structure of octadentate 3,4,3-LI(1,2-HOPO) with metal-binding oxygen atoms highlighted in red; (right) Schematic depiction of nanoparticle surface binding upon deprotonation of the 1,2-HOPO functionalities.

The Cm-doped $NaGdF_4$ formed ill-defined nanoparticles without distinct surface facets. Many nanoparticles were approximately spherical and up to 10 nm in size (Figure 2a), but several larger nanoparticles seem to have formed by coalescence. The presence of distinct necking-like features supports our hypothesis (Figure 2b). This is in accordance with reports of a low surface energy.[20] Electron diffraction patterns over large areas confirmed the hexagonal β-$NaGdF_4$ phase (Figure 2c).[21]

a. Chemical Sciences Division Lawrence Berkeley National Laboratory, Berkeley CA 94720, USA.
b. National Center for Electron Microscopy, Molecular Foundry, Lawrence Berkeley National Laboratory, Berkeley CA 94720, USA.
c. Department of Materials Science and Engineering, University of California, Berkeley, CA 94720, USA.
d. Department of Nuclear Engineering, University of California, Berkeley, CA 94720, USA.

Figure 2. (a) High-angle annular dark field scanning TEM (HAADF-STEM) image of several nanoparticles; (b) High-resolution TEM (HRTEM) image of a few nanoparticles, (c) electron diffraction pattern of a large area.

Using energy-dispersive X-ray spectroscopy (EDS), the Cm-content was quantified as being below 1% (Figure 3a, 3b). Excitation at 357 nm into the ligand band of 3,4,3-modified, Cm-doped nanoparticles results in a broad, ligand-centered emission (453 nm) derived from 3,4,3 singlet/triplet relaxation, and a narrow emission peaking at 598 nm ($^6D_{7/2} \rightarrow {}^8S_{7/2}$) arising from Cm^{3+} excited state decay (Figure 4). Excitation spectra acquired by monitoring the 598-nm signal reveal that luminescence at this wavelength responds to excitation over the range 300-360 nm (ligand), while also demonstrating a sensitivity to *f-f* transitions originating from direct excitation of the curium center between *ca*. 390-500 nm, with a peak at 397 nm assigned to $Cm^{3+}\ {}^8S_{7/2} \rightarrow {}^6I_J$ (Figure 4).[9]
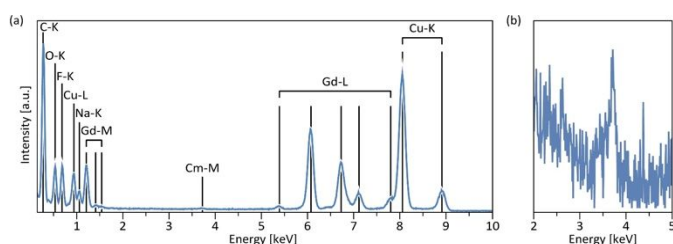
Figure 3. (a) Typical EDS spectrum of Cm-NaGdF$_4$. Cu and C peaks are due to the grid onto which the nanoparticles were deposited, whereas oxygen is a common residual gas in the microscope column; (b) Close-up of the weak Cm-M peak. The energy scale is the same as in (a), but the intensity scale has been stretched approximately 40-times.
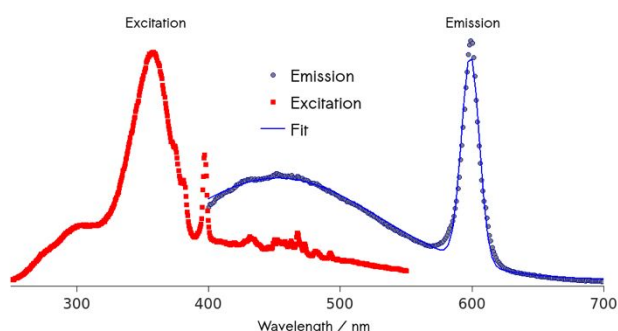
Figure 4. Steady-state photoluminescence (PL) of Cm-doped NaGdF$_4$-3,4,3 nanoparticles. Red: Excitation spectrum measured at Cm^{3+} ($^6D_{7/2} \rightarrow {}^8S_{7/2}$) emission at 598 nm. The peak at 350 nm is due to ligand absorption; the strong narrow excitation band at ca. 400 nm is the result of direct light absorption by Cm^{3+}. Blue: PL spectrum representing a summation of ligand and Cm^{3+} ion emission.

Further evidence of surface-bound ligand sensitization is seen through comparison of luminescence in the washes of the ligand-modification reactions with the nanoparticle suspension. Following a series of centrifugation/wash cycles to remove excess 3,4,3, a residual luminescence assigned to formation of the 3,4,3-Cm molecular complex is observed, with roughly 1/40th the emission intensity of the nanoparticle sample being present in the supernatant of the third wash. In addition, formation of the molecular complex in the washes is also evidenced by a significant (12 nm) shift in the Cm^{3+} emission band observed in the washes at wavelengths previously

reported for Cm^{3+}-3,4,3 (~ 610 nm),[22] which is notably distinct from the 598-nm emission wavelength of the sensitized nanocrystals (ESI). Bathochromic Cm(III) fluorescence shifts, observed with the transition from the lowest energy crystal field level of the first excited $^6D_{7/2}$ multiplet to the ground multiplet of the $^8S_{7/2}$ state, have been qualitatively associated with trends in the nephelauxetic effect.[23] The large ~16-nm shift (~450 cm^{-1}) observed upon complexation of the free Cm(III) ion by 3,4,3 in aqueous solution is characteristic of strong ligand interactions that result in diminished electrostatic repulsion effects. Within the nanocrystals, the fluorescence shift is much less pronounced (~4 nm or ~120 cm^{-1}) as the Cm ions interact with fluoride anions and the larger organic ligand is kept at the particle surface. While relatively small compared to several crystalline matrices, including Cs_2NaYCl_6,[23, 24] this shift is consistent with those observed in crystalline halides CmF$_3$ and CmCl$_3$ (~90 and ~82 cm^{-1}, respectively),[25] prior to corrections made for the crystal field splitting of the $^6D_{7/2}$ multiplet. This is further confirmation of the constrained environment of the Cm ions within the nanoparticle host.

Co-substitution with Eu^{3+} reveals that $Cm^{3+} \rightarrow Eu^{3+}$ energy transfer is also possible, with direct photoexcitation of the curium ions at 400 nm resulting in the appearance of the europium $^5D_0 \rightarrow {}^7F_2$ emission band at 612 nm. Population of europium's ^5D_J manifold presumably arises from energetic exchange between the resonant $^6D_{7/2}$ and $^5D_0$ states in curium and europium centers, respectively (ESI).

Measurements of quantum yields for the sensitization efficiency of the Cm-only system reveal a quantum yield of approximately 0.4% for the Cm^{3+} emission; factoring in ligand emission results in a total luminescence quantum yield of 1.2%. While these values are low, the curium doping levels employed here (0.075%) are far lower than those typically used in correspondent lanthanide luminescence studies. In past work, Eu^{3+} doping levels of 5% in NaGdF$_4$ with this ligand set, were used.[26] Despite the ~70-fold dopant excess used in those previous studies relative to the curium investigations here, the sensitized-europium system was found to display a quantum efficiency only an order of magnitude (Φ = 3.3%), greater than what we observe for the curium system.[26] It is worth noting that the 5% doping level used for the europium study did not place the system in a concentration-quenching regime, suggesting a significantly higher efficiency for ligand-curium energy transfer relative to the europium nanoparticle analog. This finding is consistent with earlier studies of luminescence sensitization in the 3,4,3-Cm and 3,4,3-Eu molecular complexes,[22, 27] for which respective quantum yield values of 45% and 7% had been reported in aqueous solutions buffered at physiological pH. There is, to our knowledge, no report of a better Cm sensitizing ligand than 3,4,3. However, higher brightness, larger quantum yield, and increased energy transfer efficiency could be obtained through confinement of the 3,4,3-Cm complex within a macromolecular cavity.[28] Future work will explore variations in the parameters that influence energy transfer mechanism, including different ligand architectures, both within protein matrices and in the nanoparticulate system discussed here, in order to optimize sensitization of the metal centers.

Time-dependent luminescence was investigated through pulsed excitation of the ligand band at 350 nm, with concurrent monitoring of sample emission at 598 nm (ESI). We observed a triexponential luminescence decay, with rates of k_1 = 647 s^{-1}, k_2 = 139 s^{-1}, and k_3 = 8.4 s^{-1}, with their weighted-average yielding a mean decay time of 1.26 ms (normalized weights for the respective decay phases are c_1 = 0.29, c_2 = 0.55, c_3 = 0.16). Notably, this average lifetime is much longer than those of the Cm aquo ion and the 3,4,3-Cm molecular complex (65 and 383 μs, respectively, in H_2O)[22] and more consistent with that of Cm embedded in a solid ThO_2 crystalline host matrix (1380 μs).[23] Incorporating past measurements of the 3,4,3 triplet state decay allowed determining the ligand-curium energy transfer efficiency as 0.22 (ESI). The observed multiexponential emission is likely a result of the hypersensitive Cm^{3+} photoemission, which, unlike many *f-f* transitions, is sensitive to environment. In the case of the hexagonal $NaGdF_4$ crystal system, the lanthanide/actinide ions occupy two, crystallographically-distinct sites. As a result, the lifetime of the Cm^{3+} excited state should be expected to be influenced by these distinct environments, leading to unique decay times for the $^6D_{7/2} \rightarrow$ $^8S_{7/2}$ transition. In addition, any Cm ions residing on the solvent-exposed edges of a nanocrystal will be subject to solvent-coupled deactivation paths. These ions, particularly when exposed to a protic solvent such as ethanol, would display much shorter lifetimes than their solvent-insulated counterparts residing within the nanocrystal bulk. These considerations suggest multiple distinct Cm^{3+} ions within the crystals, each with a characteristic decay time for the Cm^{3+} excited state. In the case of peripheral Cm^{3+} ions subject to protic solvent quenching, the observed decay is likely dominated by solvent quenching processes, as a result of the known ability of OH oscillators to rapidly deplete electronic excited states. In this case, solvent-exposed ions at the nanocrystal edge would have similar rates of decay, despite the existence of the two distinct *f*-element sites in this crystal host. Superposition of these three unique forms of Cm^{3+} excited-state decays at 598 nm would then be expected to result in a composite triexponential decay function.

Our experiments confirm interstitial doping of actinides in $NaGdF_4$ hosts is indeed possible, opening up avenues to synthesize radioactive, luminescent nanocrystals for therapeutic and diagnostic medical applications. While there is no radioisotope of Cm that would display adequate properties for radiotherapeutic applications, isotopes such as the trivalent ^{177}Lu and ^{225}Ac are used for targeted immuno-therapy[29-31] and are expected to exhibit coordination properties relatively similar to those of Cm within the nanoparticle hosts used in this study.[32, 33] One may envision designing systems that leverage the concerted insertion of luminescent *f*-block metals and medical *f*-block isotopes. Finally, the particular system examined in this study allows for the possibility of bio-imaging tissues at relatively low excitation powers, with the high extinction coefficient of 3,4,3 permitting relatively efficient photon absorption and Cm^{3+} luminescence relative to direct *f-f* actinide excitation.

Conflicts of interest

RJA and PA are listed as inventors on a patent application filed by the Lawrence Berkeley National Laboratory and describing inventions related to the research results presented here. The authors declare no other competing financial interests.

Notes and references

1. J.-C. G. Bünzli and C. Piguet, *Chem. Soc. Rev.*, 2005, **34**, 1048-1077.
2. X. Chen, L. Jin, W. Kong, T. Sun, W. Zhang, X. Liu, J. Fan, S. F. Yu and F. Wang, *Nat. Comm.*, 2016, **7**, 10304.
3. D. J. Garfield, N. J. Borys, S. M. Hamed, N. A. Torquato, C. A. Tajon, B. Tian, B. Shevitski, E. S. Barnard, Y. D. Suh, S. Aloni, J. B. Neaton, E. M. Chan, B. E. Cohen and P. J. Schuck, *Nat. Photonics*, 2018, **12**, 402-407.
4. M. Schubert, A. Steude, P. Liehm, N. M. Kronenberg, M. Karl, E. C. Campbell, S. J. Powis and M. C. Gather, *Nano Lett.*, 2015, **15**, 5647-5652.
5. M. H. Werts, *Sci. Progr.*, 2005, **88**, 101-131.
6. W. Zou, C. Visser, J. A. Maduro, M. S. Pshenichnikov and J. C. Hummelen, *Nat. Photonics*, 2012, **6**, 560.
7. L. J. Charbonnière, J.-L. Rehspringer, R. Ziessel and Y. Zimmermann, *New J. Chem.*, 2008, **32**, 1055-1059.
8. Z. Huang and M. L. Tang, *J. Am. Chem. Soc.*, 2017, **139**, 9412-9418.
9. M. Illemassene, K. Murdoch, N. Edelstein and J. Krupa, *J. Lumin.*, 1997, **75**, 77-87.
10. M. Irfanullah, D. K. Sharma, R. Chulliyil and A. Chowdhury, *Dalton Trans.*, 2015, **44**, 3082-3091.
11. S. Janssens, G. Williams and D. Clarke, *J. Appl. Phys.*, 2011, **109**, 023506.
12. S. Li, X. Zhang, Z. Hou, Z. Cheng, P. Ma and J. Lin, *Nanoscale*, 2012, **4**, 5619-5626.
13. J. Zhang, C. M. Shade, D. A. Chengelis and S. Petoud, *J. Am. Chem. Soc.*, 2007, **129**, 14834-14835.
14. G. Chen, C. Yang and P. N. Prasad, *Acc. Chem. Res.*, 2013, **46**, 1474-1486.
15. X. Jin, F. Fang, J. Liu, C. Jiang, X. Han, Z. Song, J. Chen, G. Sun, H. Lei and L. Lu, *Nanoscale*, 2015, **7**, 15680-15688.
16. L. C. Mimun, G. Ajithkumar, M. Pokhrel, B. G. Yust, Z. G. Elliott, F. Pedraza, A. Dhanale, L. Tang, A.-L. Lin and V. P. Dravid, *J. Mater. Chem. B*, 2013, **1**, 5702-5710.
17. Z.-L. Wang, J. Hao and H. L. Chan, *J. Mater. Chem.*, 2010, **20**, 3178-3185.
18. R. J. Abergel, P. W. Durbin, B. Kullgren, S. N. Ebbe, J. Xu, P. Y. Chang, D. I. Bunin, E. A. Blakely, K. A. Bjornstad, C. J.

Rosen, S. D.K. and K. N. Raymond, *Health Phys.*, 2010, **99**, 401-407.

19. F. Wang, R. Deng and X. Liu, *Nat. Prot.*, 2014, **9**, 1634.

20. X. Sun, B. Wang, I. Kempson, C. Liu, Y. Hou and M. Gao, *Small*, 2014, **10**, 4711-4717.

21. J. H. Burns, *Inorg. Chem.*, 1965, **4**, 881-886.

22. M. Sturzbecher-Hoehne, B. Kullgren, E. E. Jarvis, D. D. An and R. J. Abergel, *Chem. Eur. J.*, 2014, **20**, 9962-9968.

23. N. M. Edelstein, R. Klenze, T. Fanghänel and S. Hubert, *Coord. Chem. Rev.*, 2006, **250**, 948-973.

24. K. Murdoch, R. Cavellec, E. Simoni, M. Karbowiak, S. Hubert, M. Illemassene and N. Edelstein, *J. Chem. Phys.*, 1998, **108**, 6353-6361.

25. N. Stump, G. Murray, G. Del Cul, R. Haire and J. Peterson, *Radiochim. Acta*, 1993, **61**, 129-136.

26. P. Agbo, T. Xu, M. Sturzbecher-Hoehne and R. J. Abergel, *ACS Photonics*, 2016, **3**, 547-552.

27. R. J. Abergel, A. D'Aleo, C. Ng Pak Leung, D. K. Shuh and K. N. Raymond, *Inorg. Chem.*, 2009, **48**, 10868-10870.

28. B. E. Allred, P. B. Rupert, S. S. Gauny, D. D. An, C. Y. Ralston, M. Sturzbecher-Hoehne, R. K. Strong and R. J. Abergel, *Proc. Natl. Acad. Sci. USA*, 2015, **112**, 10342-10347.

29. J. G. Jurcic, M. Y. Levy, J. H. Park, F. Ravandi, A. E. Perl, J. M. Pagel, B. D. Smith, E. H. Estey, H. Kantarjian and D. Cicic, *Am. Soc. Hematology*, 2016.

30. C. Kratochwil, U. Haberkorn and F. L. Giesel, 2019.

31. G. P. Nicolas, A. Morgenstern, M. Schottelius and M. Fani, *J. Nucl. Med.*, 2019, **60**, 167-171.

32. M. G. Ferrier, E. R. Batista, J. M. Berg, E. R. Birnbaum, J. N. Cross, J. W. Engle, H. S. La Pierre, S. A. Kozimor, J. S. L. Pacheco and B. W. Stein, *Nat. Comm.*, 2016, **7**, 12312.

33. M. G. Ferrier, B. W. Stein, E. R. Batista, J. M. Berg, E. R. Birnbaum, J. W. Engle, K. D. John, S. A. Kozimor, J. S. Lezama Pacheco and L. N. Redman, *ACS Cent. Sci.*, 2017, **3**, 176-185.

<div style="background:#8fafc0; padding:10px;">

COMMUNICATION

</div>

Amplified Luminescence in Organo-Curium Nanocrystal Hybrids

Peter Agbo,[a] Alexander Müller,[b] Leticia Arnedo-Sanchez,[a] Peter Ercius,[b] Andrew M. Minor,[b,c] and Rebecca J. Abergel*[a,d]

Table of Contents Entry
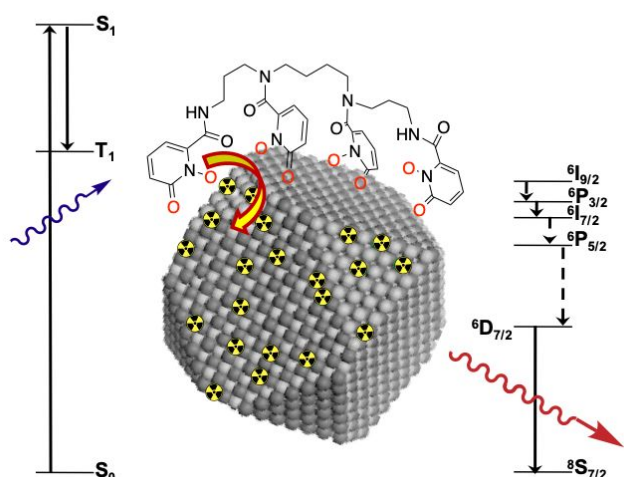
Amplified luminescence of $^{248}Cm^{3+}$ doped in a NaGdF$_4$ lattice is achieved through optical pumping of a surface-localized metal chelator, 3,4,3-LI(1,2-HOPO).

[a.] Chemical Sciences Division Lawrence Berkeley National Laboratory, Berkeley CA 94720, USA.

[b.] National Center for Electron Microscopy, Molecular Foundry, Lawrence Berkeley National Laboratory, Berkeley CA 94720, USA.

[c.] Department of Materials Science and Engineering, University of California, Berkeley, CA 94720, USA.

[d.] Department of Nuclear Engineering, University of California, Berkeley, CA 94720, USA.